CrossMark

ORIGINAL ARTICLE

Heavy metal monitoring of beach sands through environmental magnetism technique: a case study from Vengurla and Aravali beaches of Sindhudurg district, Maharashtra, India

Venkata Lakshmi Bandaru[1] · Praveen B. Gawali[1] · Pramod T. Hanamgond[2] ·
Deenadayalan Kannan[1]

Abstract Mineral magnetic, geochemical and statistical analyses were carried on surface sediments collected from Vengurla and Aravali beach, along west coast of India, premonsoon (PreM), monsoon(M) and postmonsoon (PM). Magnetic concentration parameters (χ_{lf}, ARM, SIRM and HIRM) are strongly correlated within them PreM during M and PM. Thermomagnetic analysis identifies titanomagnetite, magnetite, maghemite and hematite as the dominant magnetic mineralogy of the sediments. Strong correlation was deciphered between magnetic parameters and heavy metal (Cu, Cr, Zn and Ni) PreM and PM which obliterated in M. This shows influx of magnetic minerals and heavy metals is more in M than PreM and PM. The monsoonal influx is more haphazard and random in M because of enhanced weathering resulting in weak correlation between different mineralogical and geochemical entities. This finding outlines the efficacy of simple, rapid and non-destructive magnetic measurement which can be used as an indicator for heavy metal contamination. It can act as a proxy for measuring of heavy metal content in the coastal and beach environment.

Keywords Mineral magnetic · Heavy metal · Statistical · Geochemical · Beach · West coast

✉ Venkata Lakshmi Bandaru
   bvlakshmi@iigs.iigm.res.in

1   Indian Institute of Geomagnetism, New Panvel,
    Navi Mumbai, Maharashtra, India

2   Department of Geology, GSS College, Belgaum, Karnataka,
    India

Introduction

Investigating the compositional properties of rocks, sediments and soils using mineral magnetic measurements is nowadays a routine form of analysis (Thompson and Oldfield 1986; Walden et al. 1999; Maher and Thompson 1999; Oldfield 1999a, b). The technique has been applied to various depositional environments (e.g. Arkell et al. 1983; Oldfield et al. 1985, 1999; White et al. 1997; Walden et al. 1995, 1997; Schmidt et al. 1999; Wheeler et al.1999). Many have also explored the relationship between mineral magnetic measurements and chemical/physical properties of sediments and soils (Oldfield et al. 1985; Oldfield and Yu 1994; Clifton et al. 1997, 1999; Chan et al. 1998; Petrovsky et al. 1998; Xie et al. 1999, 2000; Booth 2002). These investigations have revealed mineral magnetic measurements to be a suitable tool for determining sediment provenance (Oldfield and Yu 1994; Booth 2002; Gawali et al. 2010), sediment transport pathways (Lepland and Stevens 1996), which also serves as a proxy for geochemical, radioactivity, organic matter content and particle size data (Bonnett et al. 1988; Oldfield et al. 1993; Hutchinson and Prandle 1994; Clifton et al. 1997, 1999; Xie et al. 1999, 2000; Zhang et al. 2001). The environmental magnetic method has been successfully utilized for coastal investigations that include sediment sources and transport pathways, and determining contamination of heavy metals in estuaries and tidal flats (Oldfield et al. 1985; Lees and Pethick 1995, Zhang et al. 2001). Environmental magnetic methods (magnetic fingerprinting and magnetic inclusions) are extensively used to resolve various coastal research problems including investigating particulate pollution, to identify and characterize the sediment sources and to examine sediment dynamics in coastal

environments (Maher et al. 2008, 2009; Maher and Kinnersely 2010, 2011; Maher and Hatfield 2009).

Recently environmental magnetic methods have been used to map the distribution of heavy minerals and to assess their degree of sorting (Cioppa et al. 2010). Studies by Hatfield et al. (2010) used environmental magnetics to identify and monitor areas of erosion and deposition on a coastal foreland. Gallaway et al. (2012) investigated the mechanism of magnetic mineral transport and highlighted the role of burial mechanism in magnetite enrichment in swash zones. However, the processes controlling magnetic mineral enrichment and transport in coastal depositional environments are not yet well enough understood to make detailed predictions about their distribution patterns and to draw deductions on the governing local hydrodynamic conditions. This paper presents magnetic and geochemical analyses of beach sediments along Vengurla and Aravali beaches of Sindhudurg district, Maharashtra. The purpose of this investigation is to critically examine the potential of applying mineral magnetic parameters as a proxy for heavy mineral concentration.

Study area

The two beaches, Vengurla and Aravali, stretch for more than 8 km in length and are located in the Sindhudurg district, the southernmost part of the Maharashtra state (Fig. 1). These beaches are microtidal and are under the influence of semi-diurnal tides. They are part of the Konkan Coast, which has morphological features distinct from those of the rest of the Indian coast (Chandramohan et al. 1992). The entire coastal stretch of Konkan was tectonically active during the Miocene–Pliocene period. Since then, exogenetic processes are seen to be dominating (Tandale 1993). The study area has Vengurla Beach (Vengurla-Kepadevi, Stations 1–4; width 30–150 m) and Aravali Beach (Mochemad-Kerwada, Stations 5–9; width 50–185 m). The rainfall ranges between 300 and 470 cm/year, and wave height reaches up to 1.0 m, with an average wave period of 5 to 6 s. The predominant wave activity is of plunging type with multiple breakers.

The geology of the area (Fig. 1) consists of banded hematite quartzite, varieties of schist, and granitic rocks (Deendar 2003). Vengurla has a moderate to bold relief with hills and deep valleys. It has a coastline on its western side with a NNW–SSE trend. The coastline to the north of Vengurla is rocky, but it is not so in the south. River Karli flows from east to west and borders the northern part. River Talvada flows from north-east to south-west and joins the sea at Mochemad. River Redi, which marks the southern border of Vengurla, has a north–south flow on the eastern side and abruptly changes to an east–west direction near Shiroda to join the sea. The general trend of the major rivers in the area is from east to west, where they join the Arabian Sea. Two more rivers join the sea at the Vengurla port hill, situated on the northern and southern sides of the hill. These rivers have a major east–west trend. The important rock units in the region are banded hematite quartzite, quartzite, and schist (amphibolite and garnet), as well as granitic rocks. The area is structurally disturbed and influences the geology and the drainage pattern to a large extent (Deendar 2003). Faulting is a major factor influencing the deformation and rock alterations, facilitating the formation of residual ore deposits and iron ore containing rocks in the area. The sustainable iron ore deposit of Redi, thus formed, has supported large-scale mining operations over a long period, with workable reserves of about 48 metric tons (Hiremath 2003).

Materials and methods

The upper 3–4 cm of surface sediment samples were collected from the beaches seasonally premonsoon (PreM; May 2003), during monsoon (M) (July 2003), and postmonsoon (PM; November 2003) at nine stations (3–4 samples from each station) along Vengulra and Aravali beaches of the study area (Fig. 1). The samples were collected in a polythene bag. In the laboratory, sample were dried at 40 °C, weighed and packed tightly into 8 cm^3 plastic bottles before the measurements. Initial, low-frequency, mass-specific magnetic susceptibility (χ_{lf}) was measured using MFK1-FA Kappa bridge (AGICO). The percentage frequency dependence susceptibility χ_{fd} % is calculated using the formula χ_{fd} % = ($\chi_{lf} - \chi_{hf}$)/$\chi_{lf} \times 100$. Anhysteric remanent magnetization (ARM) was measured after demagnetization in an alternate field (AF) field of 100mT, inducing Direct Current biasing field of 0.05 mT using Molspin AF demagnetizer and was measured on the Molspin magnetometer. Isothermal remanent magnetization (IRM) acquisition curves in steps from 10 to 1000 mT; backfield application to the saturation isothermal remanent magnetization (SIRM) and evaluation of the remanent coercive force (Hcr) were performed using Molspin pulse magnetizer. After a sample has acquired an IRM it is often possible to (partially) demagnetize the sample by exposing it to a magnetic field of reversed direction. Such a partial demagnetization can yield information about the ease of remanence acquisition, or the coercivity of a sample. The results are expressed as S ratio ($S_{300} = $ IRM$_{-300}$/SIRM) and hard isothermal remanent magnetization (HIRM = SIRM-IRM$_{-300}$, being IRM$_{-300}$

the acquired IRM at a backfield of 300 mT). In order to identify magnetic mineralogy, temperature dependent magnetic susceptibility (χ–T curves) using AGICO KLY-4S Kappabridge attached to CS-3/CSL furnaces and SIRM thermal demagnetization measurements using a MMTD-80 thermal demagnetizer (Magnetic Measurements Ltd.) were carried out on 10 samples.

Geochemical analysis for some samples was performed using X-ray fluorescence (XRF) for determining elemental concentrations. For sample preparation 8 gm of dried sediment was ground, of which 4 g was used for geochemical analysis using Spectro XEPOS XRF spectrometer (AMETEK) by the Turboquant-Powders method (http://www.ametek.com). For analysis, the standard MCA calibration sample from Fluxana (http://www.fluxana.com) was used. The whole set of data (environmental magnetic and geochemical data) in this study was analyzed by multivariate statistical methods, including correlation matrix. All the data processing for statistical analysis was done with the statistical software SPSS for Windows (Ver. 16).

Results and discussion

Environmental magnetic analysis

Magnetic concentration parameters χ_{lf}, SIRM and ARM are sensitive to changes in the concentration of magnetic minerals (e.g. Anderson and Rippey 1988; Lanci et al. 1999; Geiss et al. 2004). Superparamagnetic (SP) particles record high χ_{lf} and relatively high values for multidomain (MD) grains (Thompson and Oldfield 1986). ARM is more sensitive than SIRM to single domain (SD) grains (Turner 1997). The total χ of a sample is the sum of the ferrimagnetic, paramagnetic or diamagnetic contributions, whereas SIRM and ARM are independent of paramagnetic minerals. SIRM is highly dependent on the make-up of different types of magnetic minerals (e.g., magnetite has measurements two orders of magnitude higher than hematite). Therefore, all three parameters should be studied simultaneously to infer changes in magnetic concentration.

Mineral magnetic data for PreM, M, and PM are presented in Fig. 2. The χ_{lf} values show considerable variation

Fig. 1 a Location map and Geology (modified after Deendar 2003) of the study area. REDI is the location of iron ore deposit
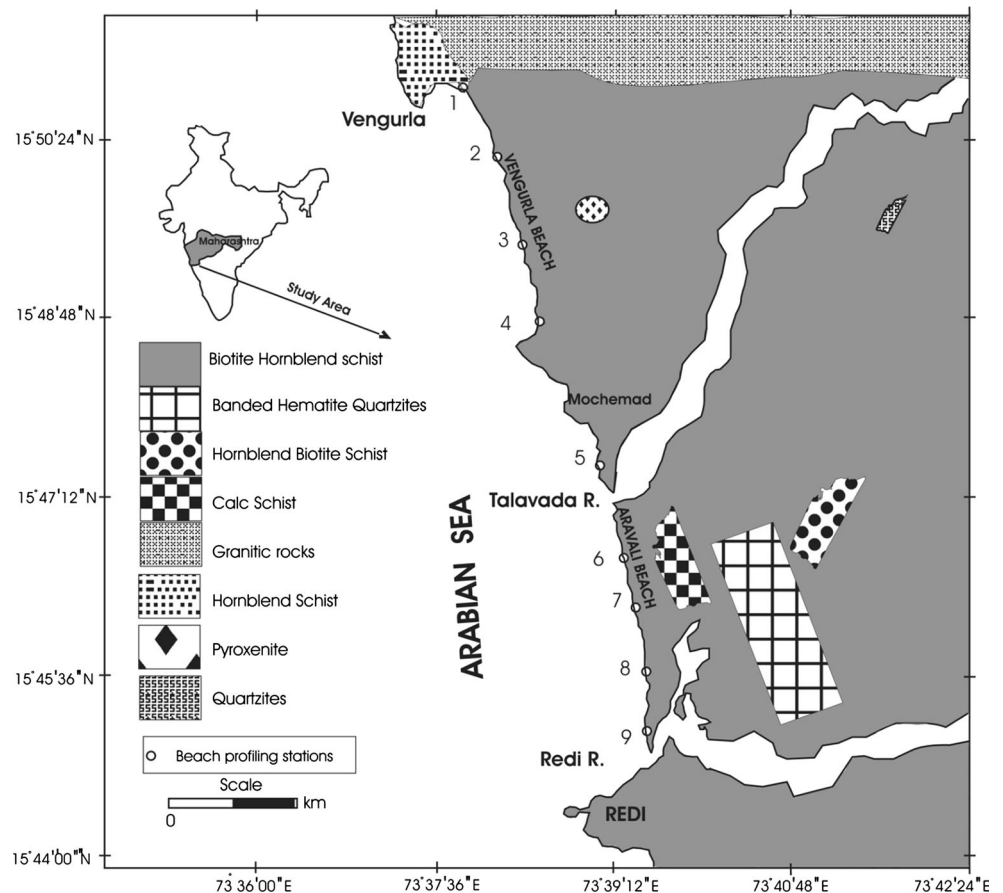
PreM (0.02–2.05 × 10^{-7} m³/kg), during M (0.02–2.17 × 10^{-7} m³/kg) and PM (0.12–6.03 × 10^{-7} m³/kg) exhibiting low concentration of magnetic minerals at all stations, except at 8 and 9 stations where a sudden rise is observed PreM, during M and PM (Fig. 2a). Samples from PreM, M and PM of stations 1 and 2 indicate high ARM values (Fig. 2c, 1.5 × 10^{-5}, 1.20–1.74 × 10^{-5} and 0.94–1.57 × 10^{-5} Am³/kg). Samples from stations 3, 4, 5 and 6 contain moderate and low to moderate ARM (PreM-0.28–0.58 × 10^{-5}, M-0.17–0.86 × 10^{-5} and PM-0.19–0.99 × 10^{-5} Am³/kg) values. Stations 7, 8 and 9 exhibit variable concentration of stable SD magnetic minerals with moderate to very high ARM values in all three seasons. SIRM values for PreM, M and PM samples from stations 1–7 indicate very low to low concentrations of all remanence-carrying magnetic minerals (Fig. 2b). By

contrast, stations 8 and 9 show SIRM concentration to be moderate PreM (581 and 564 × 10^{-5} Am³/kg), low to moderate in M (80 and 996 × 10^{-5} Am³/kg) and low to moderate PM (31 and 690 × 10^{-5} Am³/kg).

Changes in magnetic mineralogy can be determined by using IRM acquisition curves, H_{cr}, χ–T curves, SIRM thermal demagnetization, S ratio and Hard IRM. S ratio is a dimensionless parameter that discriminates content of ferrimagnetic with respect to antiferromagentic minerals; values close to 1 correspond to the predominance of ferrimagnetic minerals. Magnetic minerals in sediments can also be identified as soft and hard fractions. The hard fraction has high coercivity and can be used to estimate the total concentration of canted antiferromagnetic minerals (hematite; Oldfield and Richardson 1990). The variation of S ratio (Fig. 2h) is from 0.4 to 0.8, 0.2 to 0.8 and from 0.3
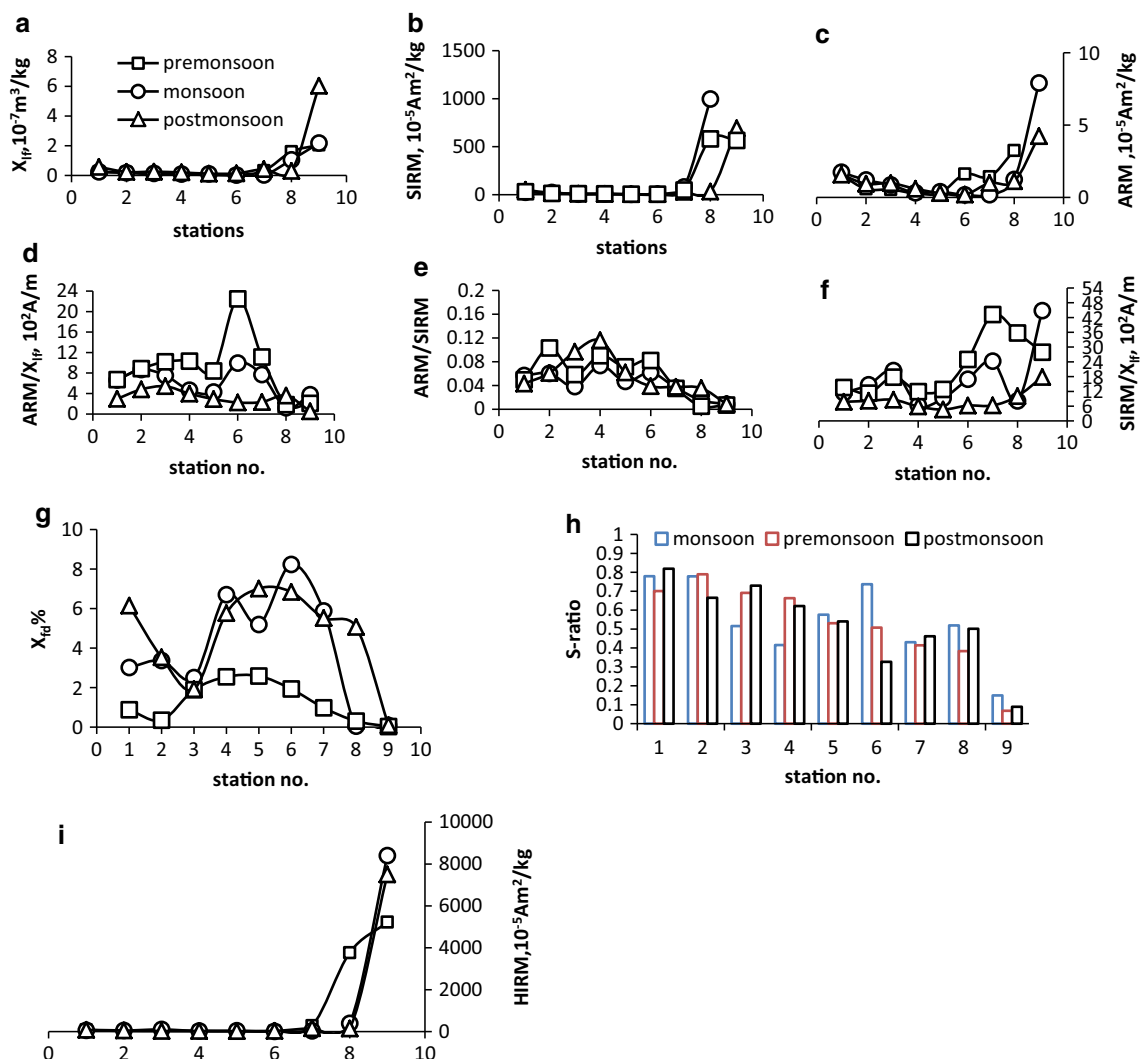

Fig. 2 a–i Plot of χ_{lf}, SIRM, ARM, ARM/χ_{lf}, ARM/SIRM, SIRM/χ_{lf}, χ_{fd} %, S ratio and HIRM vs. sampling stations

to 0.8 for PreM, M and PM with an average value of 0.5. Hard IRM varies from 20 to 3767 $\times$ 10^{-5} Am^3/kg PreM, 10 to 8401 $\times$ 10^{-5} Am^3/kg during M and from 22 to 7498 $\times$ 10^{-5} Am^3/kgPM. Figure 2i shows that there is a lower concentration of HIRM up to station 8, whereas at station 9 higher concentrations exist. This gives an idea that soft magnetic minerals are present up to station 8 and a subordinate hard component at station 9. Figure 3a–f shows typical curves for IRM acquisition, back field and χ–T curves. For most samples, <95 % of saturation is achieved at ~200 mT, indicating a predominantly low coercivity mineral contribution (Fig. 3a).This is supported by H$_{cr}$ values ranging from 30 to 60 mT (Fig. 3b). All the samples from stations present a curie temperature from 580 to 620 °C suggesting the dominance of magnetite and maghemite minerals. At stations 3 and 9, there is a small

decrease of χ between 250 and 350 °C and increasing thereon with a peak at around 450 °C, suggesting titanomagnetite.

Samples collected at Station 1, M and PreM display SIRM decrease at unblocking temperature (T$_b$) of about 300, 400 and 675 °C (Fig. 4a). This could be due to titanomagnetite and hematite. Samples collected at station 2 during the M and PM campaigns display a spectra of decrease in SIRM, with temperature reaching a T_b of about 300, 580, and 680 °C (Fig. 4b), indicating titanomagnetite, magnetite and hematite, respectively. The SIRM thermal demagnetization of samples collected at Station 3, PM and PreM display a distinct change in behavior from 200 to 400 °C (Fig. 4c). A drop in SIRM occurs in the PM sample at 250 °C, after which a gradual decrease is seen to about 675 °C. This could be due to titanomagnetite and hematite.

Fig. 3 Typical examples of **a** acquisition of isothermal remanent magnetization; **b** backfield demagnetization and **c–f** temperature dependence of magnetic susceptibility (χ–T curves)
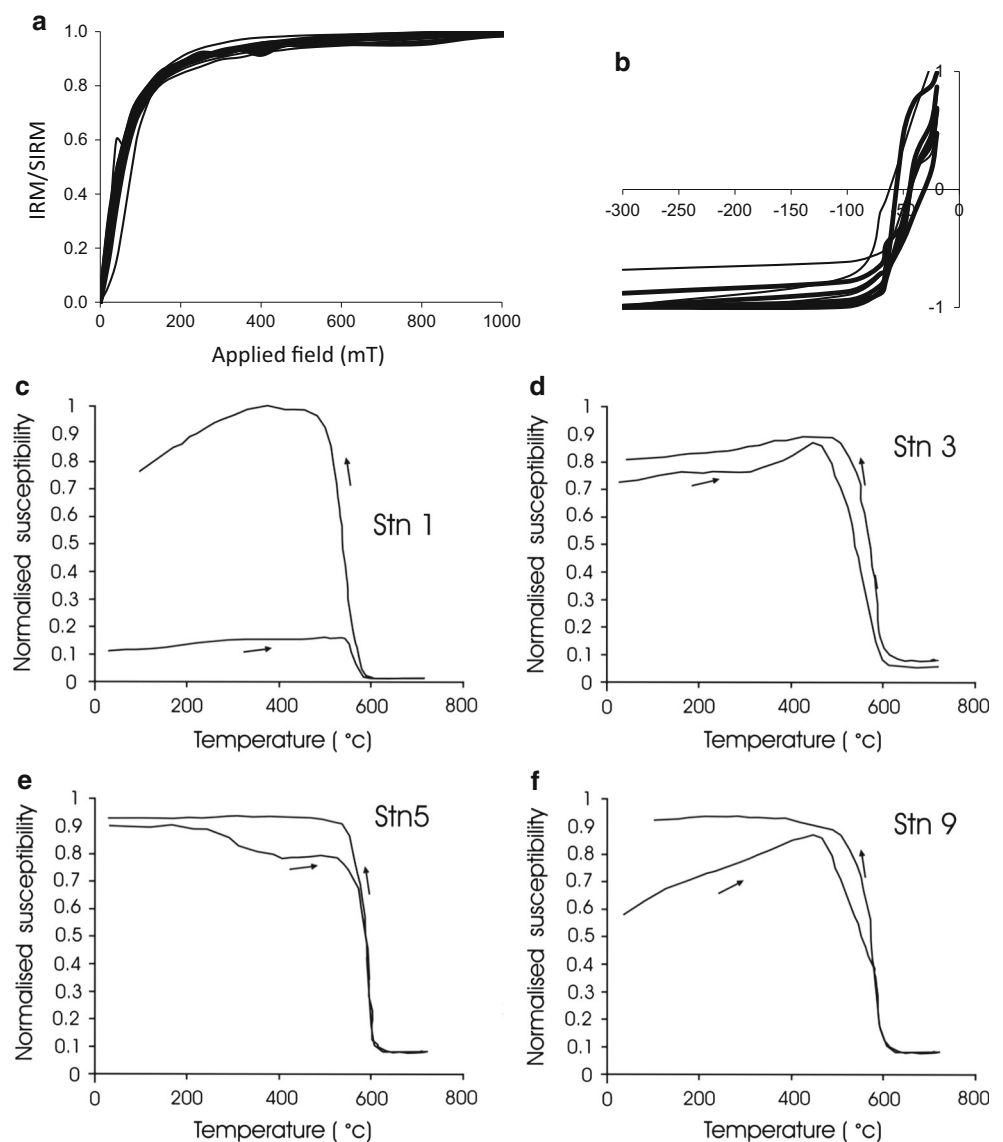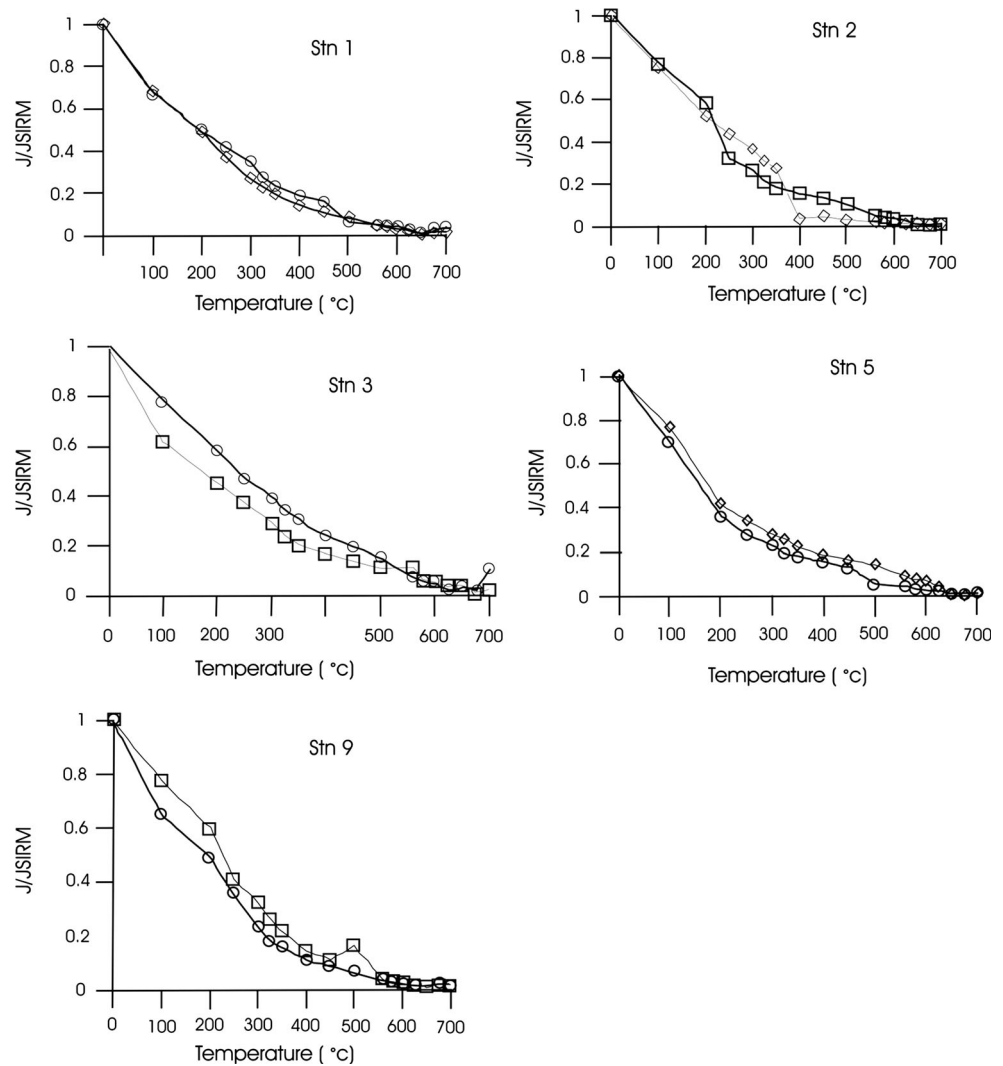
Fig. 4 Thermal demagnetization of selected samples for PreM, M and PM. *Open circles, squares* and *diamonds* represent M, PM and PreM, respectively

The PreM sample has one magnetic mineral phase with (T_b) of about 400 °C, denoting the presence of titanomagnetite, and the other is magnetite with a T_b of about 580 °C. On demagnetization, the sample collected in M season at Station 5 shows a T_b of around 450 °C and 675 °C (Fig. 4d), denoting the presence of titanomagnetite and hematite, respectively. The sample collected at Station 9, during M season is seen to display two phases of magnetic mineralogy (Fig. 4e), one with a T_b at 420 °C (titanomagnetite) and the other with a T_b that lies between 580 and 600 °C. This could be magnetite. The PM sample at Station 9, displays a T_b of 580 °C, *i.e.,* magnetite (Fig. 4e). Overall the magnetic mineralogy of the sediments is variable in Titanomagnetite, magnetite and hematite.

Changes in magnetic grain size and the interparametric ratios of ARM/χ_{lf}, ARM/SIRM and SIRM/χ_{lf} can be used for grain size interpretation. The ARM/χ_{lf} ratio can be used to distinguish particle size of sediments in general

and magnetic minerals in particular (Banerjee et al. 1981). Low ratios indicate coarse grain sizes, whereas high values suggest fine magnetic grain sizes. At stations 1, 2, 3, 4 and 6, ARM/χ_{lf} values (Fig. 2d) show increasing trend except at station 5 and then decreasing trend at 7, 8 and 9 is seen PreM. In M, initially there is a decreasing, then increasing and again a decreasing trend. PM, there is a increasing and decreasing trend. The ARM/SIRM ratio is the best estimator of changes in magnetic grain size because neither of the two parameters depends on paramagnetic minerals (Turner 1997). The ARM/SIRM (Fig. 2e) values for PreM and M are seen to fluctuate up to station 5 and then exhibit decreasing trend. There is an increasing trend up to station 4 and then decreasing trend PM (Fig. 2e). The decreasing trend of ARM/SIRM values towards Aravali stations signifies increase in grain size (coarser) as compared to finer at Vengurla stations. The SIRM/χ_{lf} displays high values where smaller, SD grains are present (Peters and Dekkers 2003; Heider et al. 1996).

Table 1 Descriptive statistics of various magnetic parameters

χ_{lf}	PreM	M	PM	χ_{fd} %	PreM	M	PM
Mean	0.508	0.4436	0.9157	Mean	1.2742	3.8899	4.6534
SD	0.75963	0.72244	1.92136	SD	0.98248	2.84195	2.35185
Minimum	0.02	0.02	0.12	Minimum	0.03	0.05	0.09
Maximum	2.05	2.17	6.03	Maximum	2.58	8.23	7.01
ARM	PreM	M	PM	SIRM	PreM	M	PM
Mean	1.2225	1.5537	1.2096	Mean	140.6002	130.4547	94.0682
SD	0.93826	2.44466	1.20900	SD	245.53723	325.54145	224.30494
Minimum	0.28	0.17	0.19	Minimum	4.40	2.86	4.87
Maximum	3.24	7.91	4.23	Maximum	580.94	996.24	690.84
S ratio	PreM	M	PM	HIRM	PreM	M	PM
Mean	0.5276	0.5446	0.5284	Mean	1054.3744	1011.4886	893.8641
SD	0.22050	0.20462	0.22105	SD	1986.33750	2773.78139	2477.41794
Minimum	0.07	0.15	0.09	Minimum	21.71	10.06	22.29
Maximum	0.79	0.78	0.82	Maximum	5224.02	8401.64	7498.92
ARM/χ	PreM	M	PM	ARM/SIRM	PreM	M	PM
Mean	9.1118	6.0415	3.1910	Mean	0.0558	0.0441	0.0556
SD	6.06515	2.76010	1.46677	SD	0.03495	0.02185	0.03314
Minimum	1.82	1.20	0.51	Minimum	0.01	0.01	0.01
Maximum	22.48	9.94	5.41	Maximum	0.10	0.07	0.12

PreM premonsoon, *M* monsoon, *PM* postmonsoon. Units: $\chi_{lf} = 10^{-7}$ m^3/kg, ARM $= 10^{-5}$ Am^2/kg, SIRM $= 10^{-5}$ Am^2/kg, ARM/$\chi = 10^2$ A/m, and HIRM $= 10^{-5}$ Am^2/kg

However values >70 kA/m are considered to be an indicator of the iron sulfide greigite (Fassbinder and Stanjek 1994; Blanchet et al. 2009; Roberts et al. 2011). SIRM/χ_{lf} varies from 11 to 43, 6–45 and 4.6–17.8 kA/m PreM, M and PM, respectively (Fig. 2f). χ_{fd} %, which is an indicator of SP grains, can also be used as a proxy for grain size. Values of χ_{fd} % <4.0 % indicates virtually no SP and dominant MD and SSD grains while χ_{fd} % >10.0 % reflects high content of SP grains (Dearing 1999). χfd % is seen to vary from 0.03 to 2.6 % with an average value of 1.27 % PreM; 0.05 to 8.2 % with an average of 3.9 % in M and 0.09–7.0 % with an average of 4.7 % PM (Fig. 2g). Mean values of χ_{fd} % are lesser than 10 % and, therefore, indicate that SP minerals are not dominant in these samples. All the above referred grain size parameters suggest these beach sediments are dominated by SD and MD minerals.

Descriptive statistics and inter-parametric correlations for beach sediments are presented in Tables 1 and 2. The mass-specific susceptibility (χ_{lf}), ARM and SIRM show notable increase PM, during M and PreM, respectively. The mean values of ARM/SIRM, S ratio and HIRM do not show any significant change in PreM, M and PM periods.

ARM/χ_{lf} values for PM are relatively high suggesting presence of coarser and larger grain size sediments relative to PreM samples. χ_{fd} % mean values during PreM, M and PM fall in the range of SD and MD. The inter-parametric correlations (Table 2) indicate significant positive correlation (supported by P values at cut off level 0.05) between χ_{lf} and ARM PreM; and good correlation in M and PM. χ_{lf} also show good correlation with SIRM and HIRM preM during M and PM.

Geochemical analysis

Figure 5 depicts the concentration of abundant (Fe, Mg and Al) and heavy metals (Cu, Cr, N and Zn). The concentration ranges of abundant elements Al, Fe, and Mg are 1.2–2.1, 0.77–18.88, and 0.20–0.60 % PreM; 0.70–3.36, 0.18–0.72 and 1.31–2.16 % for M and 0.77–17.68, 0.27–1.05 and 1.33–2.25 % PM, respectively (Fig. 5a, c and e). As can be deciphered from Fig. 5a, c and e, Fe is more PreM and PM for station 8 and 9 of Aravali beach. The concentrations of heavy metals in beach sediments are Cu: 4.1–18.6 ppm (PreM), 3.5–8.4 (M) and 3.2–15.1 ppm (PM); Cr: 21.9–286.6 ppm (PreM),

Table 2 Correlation coefficient values of mineral magnetic parameters

	χfd %	ARM	SIRM	S ratio	HIRM	ARM/χ	
Premonsoon							
χfd %	**−0.719** (0.029)						
ARM	**0.798** (0.010)	**−0.857** (0.003)					
SIRM	**0.983** (0.000)	−0.664 (0.051)	**0.685** (0.042)				
S ratio	**−0.818** (0.007)	0.403 (0.282)	−0.635 (0.066)	**−0.779** (0.013)			
HIRM	**0.994** (0.000)	−0.654 (0.056)	**0.759** (0.018)	**0.980** (0.000)	**−0.841** (0.005)		
ARM/χ	**−0.694** (0.038)	0.555 (0.120)	−0.630 (0.069)	**−0.681** (0.044)	0.340 (0.370)	−0.659 (0.054)	
ARM/SIRM	**−0.827** (0.006)	0.573 (0.107)	−0.634 (0.067)	**−0.830** (0.006)	**0.778** (0.014)	**−0.807** (0.009)	0.623 (0.073)
Monsoon χfd %	**−0.748** (0.020)						
ARM	**0.926** (0.000)	−0.643 (0.062)					
SIRM	**0.927** (0.000)	−0.558 (0.119)	**0.983** (0.000)				
S ratio	**−0.678** (0.045)	0.344 (0.364)	−0.627 (0.071)	**−0.721** (0.028)			
HIRM	**0.916** (0.001)	−0.532 (0.141)	**0.978** (0.000)	**0.999** (0.000)	**−0.729** (0.026)		
ARM/χ	**−0.791** (0.011)	**0.769** (0.015)	−0.630 (0.069)	−0.651 (0.058)	0.625 (0.072)	−0.638 (0.065)	
ARM/SIRM	**0.685** (0.042)	−0.357 (0.346)	**0.815** (0.007)	**0.852** (0.004)	−0.640 (0.063)	**0.860** (0.003)	−0.607 (0.083)
Postmonsoon							
χfd %	**−0.728** (0.026)						
ARM	**0.957** (0.000)	**−0.774** (0.014)					
SIRM	**1.000** (0.000)	**−0.724** (0.027)	**0.955** (0.000)				
S ratio	**−0.719** (0.029)	0.326 (0.393)	−0.538 (0.136)	**−0.724** (0.028)			
HIRM	**0.998** (0.000)	**−0.726** (0.027)	**0.940** (0.000)	**0.998** (0.000)	**−0.747** (0.021)		
ARM/χ	**−0.691** (0.039)	0.055 (0.887)	−0.579 (0.102)	**−0.692** (0.039)	**0.801** (0.009)	**−0.689** (0.040)	
ARM/SIRM	−0.550 (0.125)	0.156 (0.688)	−0.552 (0.124)	−0.558 (0.118)	0.629 (0.070)	−0.540 (0.133)	**0.766** (0.016)

Correlation is significant (in bold) at the 0.05 level and derived using SPSS software. The *p* values of significant correlation are produced in brackets

25.3–100.2 ppm (M) and 17.6–310.7 (PM); Ni: 5.8–20.7 ppm (PreM), 5.2–10.2 ppm (M) and 5.6–17.8 ppm (PM); Zn: 6.2–37.9 ppm (PreM), 5.3–16.9 (M) and 5.6–132.8 ppm (PM) (Fig. 5b, d and f). Cr is more dominant in stations 8 and 9 PreM and PM periods than M.

Correlation analysis was carried out to identify relationship, if any, that exists between magnetic parameters and heavy metal concentration. The concentrations of four heavy metals (Cu, Cr, Ni and Zn) are plotted against χ_{lf}, SIRM and HIRM for three seasons (Figs. 6, 7), where correlation coefficients between the heavy metal concentrations and magnetic susceptibility are also given. Table 3 shows Pearson's correlation coefficient values (*r*) between mineral magnetic parameters and heavy metals for PreM, M and PM periods. Significant correlations (supported by P values at cut off level 0.05) exist between χ_{lf}, SIRM, HIRM and heavy metal concentration PreM and PM (Figs. 6a–h, 7e–h). However, each of these relationships is absent in M. No significant correlation between any of the mineral magnetic and heavy metal concentration is seen during M. ARM shows good correlation with heavy metal

concentration only PM. S ratio shows a strong negative correlation with heavy metal concentration PreM and PM (Fig. 7a–d).

The Sindhudurg beaches, just like other Konkan beaches, receive sediments from a number of sources. The bedrock is broken into smaller fragments by water, wind and other climatic processes operative through physical comminution and chemical weathering. Hydrodynamic processes are an important source of placer formations across the beaches (Kurian et al. 2000) along with alongshore and cross-shore movement of sediments (Chandrasekar et al. 2003). Li et al. (2002) consider sediment transport processes in the swash zone are important to beach morphology and shoreline stability. Heavy mineral accumulation depends on source and is controlled by shoreline configuration and seasonal wave climate (Chandrasekar et al. 2005). Strong winnowing action of waves is responsible for heavy mineral concentration rather than the selective transport through alongshore currents (Hegde et al. 2006). The Vengurla and Aravali beaches are exposed to variable

Fig. 5 Variation of Heavy metal concentration Iron (Fe), magnesium (Mg), Aluminum (Al), Copper (Cu), Chromium (Cr), Nickel (Ni) and Zink (Zn) at different stations for PreM, M and PM. **a**, **b** Fe, Mg, Al, Cu, Cr, Ni and Zn for PreM; **c**, **d** Fe, Mg, Al, Cu, Cr, Ni and Zn for M and **e**, **f** Fe, Mg, Al, Cu, Cr, Ni and Zn for PM
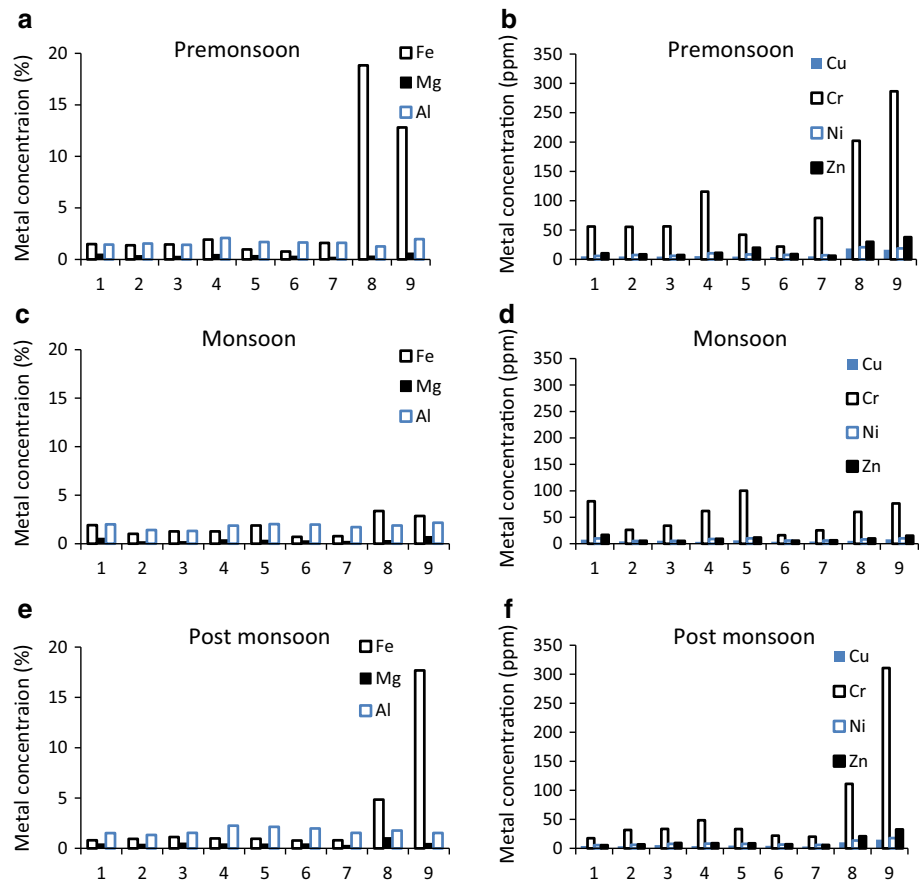

environmental conditions which are reflected in the detrital pattern of accumulation and/or erosion. Though they seem to share similar geochemical realm, the heavy metal as well as abundant element characteristics sometimes are seen to be at variance with each other. The heavy metal concentration shares significant correlation with magnetic parameters PreM and PM. This correlation is completely lost during M. S ratio, on the other hand, shows a strong negative correlation with heavy metals PreM and PM. Overall the Aravali beach has more concentration of magnetic minerals than the Vengurla beach. The strong association of heavy metals with magnetic mineral concentration indicates their interrelationship. Ti and Fe are reckoned to have been released from the banded hematite formations. The hinterland is likely having some deposits of chromite. Our results underline the presence of Cr in the beach samples, especially towards the end of Aravali beach. Gujar et al. (2010) studied heavy mineral placers from Vijaydurg to Redi and found opaques to contain ilmenite (43.07 % in areas of significant concentration and 11.02 % in areas of localized concentration), magnetite (58.15 and 8.72 %) and chromite (up to 10.09 %). The metamorphic rocks of the

hinterland contribute substantially to the sands of the beaches, apart from the Deccan traps. The significance of temperature dependent susceptibility and SIRM measurements backs our contention regarding the presence of both magnetite and hematite along the Vengurla and Aravali beaches. The pathways for antiferromagnetic minerals coming from the hinterland are obvious. The metamorphic rocks in the vicinity of these two beaches are brought down in remnants through wear and tear during the transit. The iron ore mines are also found to be active around the Redi area. The ore material spills during the transportation adding the antiferromagnetic material to these beaches. But, the presence of magnetite and titano magnetite can be attributed to the longshore currents prevailing along these beaches, which bring the eroded particles from the Deccan traps.

The Vengurla–Aravali beaches are perceived to receive their detrital input from the surrounding region. The hinterland is seen to be dominated by hematitic mineral assemblage. The present mineral magnetic study provides a strong support for this, which brings out the domination of antiferromagnetic minerals. It must also be noted that oxidation of magnetite and Ti-magnetite can result in the

Fig. 6 Variation of Copper (Cu), Chromium (Cr), Nickel (Ni) and Zink (Zn) versus magnetic mineral concentration parameters: magnetic susceptibility (χ) and saturation isothermal remanent magnetization (SIRM). **a–d** Cu, Cr, Ni and Zn versus χ_{lf}; **e–h** Cu, Cr, Ni and Zn versus SIRM. *Squares*, *open circles* and *filled* triangles represent PreM, M and PM, respectively. NS-not significant
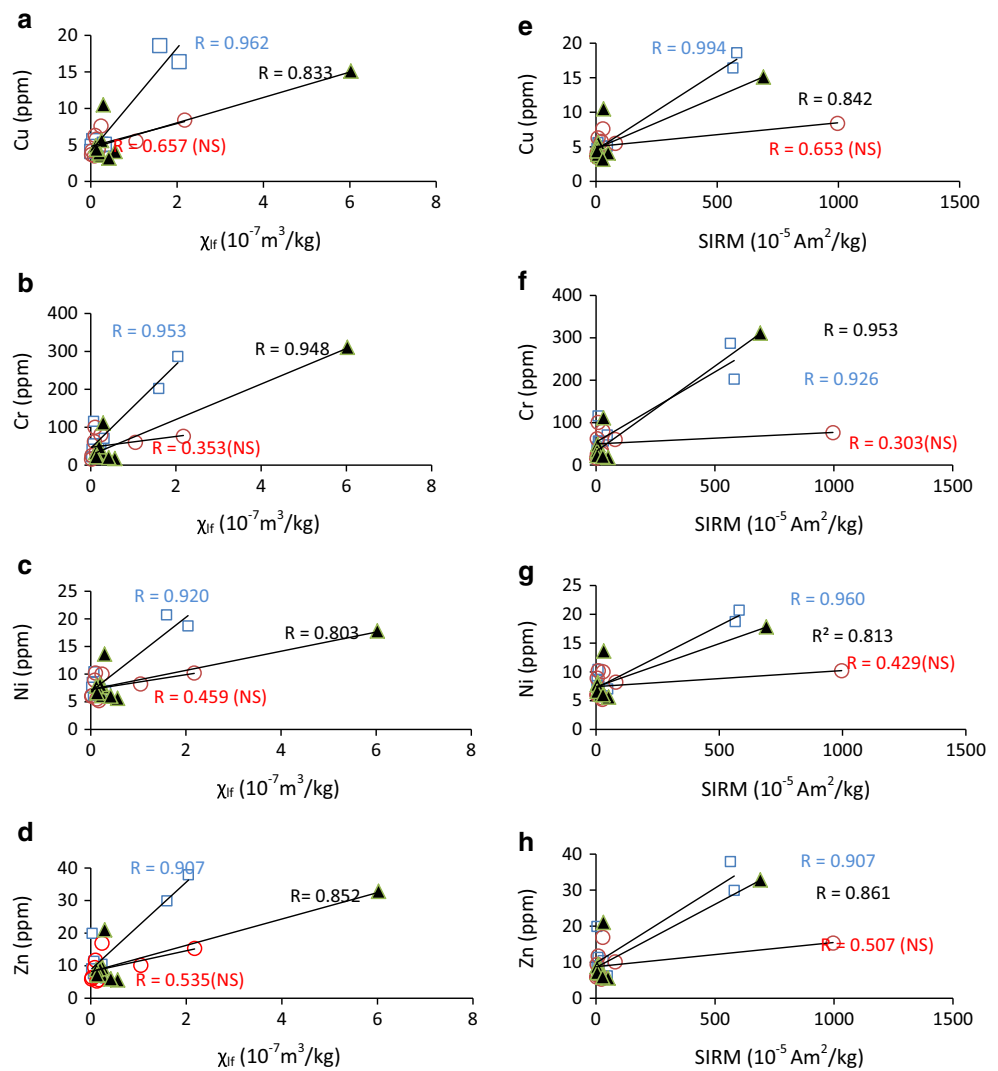

formation of maghemites (Barron and Torrent 2002) by the process called maghemitization (Dunlop and Ozdemir 1997). The small size of authigenic magnetite crystals can be oxidized in periods when the soil is aerated (van der Marel 1951; Schwertmann and Heinemann 1959; Murad and Schwertmann 1993) to form maghemite. Maghemite can form from magnetite because of their structural similarities (Fasiska 1967). Maghemite is relatively abundant in well-aerated tropical soils containing high hematite/goethite ratio (Fontes and Weed 1991; da Costa 1996), which is in appreciable abundance around Vengurla–Aravali beaches. Maghemitization is a widespread process reported from different environments and in natural samples magnetic evidence for maghemite with a thermal stability around 597 °C has been reported from basaltic rocks (Gee and Nakanishi 1995; Chévrier et al. 2006). The high heavy metal concentration and Fe preM and PM at Aravali beach reveals that source is from south

of Aravali beach in which sediment transport, delivery and flux play a major role in this process. Iron ore deposits are transported from near Redi beach which is situated to the south of Aravali beach (Gawali et al. 2010). Iron ore in the Redi and surrounding areas is associated with banded ferruginous quartzites and Precambrian ferruginous phyllites. The iron ore consists essentially of hematite and partly of magnetite, limonite, and goethite, which occur as reefs and lentoid bodies. This further strengthens our results regarding source of the sediments. Our studies also bring out the interrelationship of heavy metals and magnetic parameters. Thus, the geology and geomorphology of the area plays a big role in accumulation of sands at these beaches, which are reworked by the prevalent wind and current regime.

The beach environment all over the world is under stress and being polluted by heavy metals. The fast and inexpensive magnetic measurements can be used to screen

Fig. 7 Variation of Copper (Cu), Chromium (Cr), Nickel (Ni) and Zink (Zn) versus magnetic mineral concentration parameters: *S* ratio and Hard isothermal remanent magnetization (HIRM). **a–d** Cu, Cr, Ni and Zn versus *S* ratio; **e–h** Cu, Cr, Ni and Zn versus HIRM.. *Squares, open circles* and *filled triangles* represent PreM, M and PM, respectively. NS-not significant
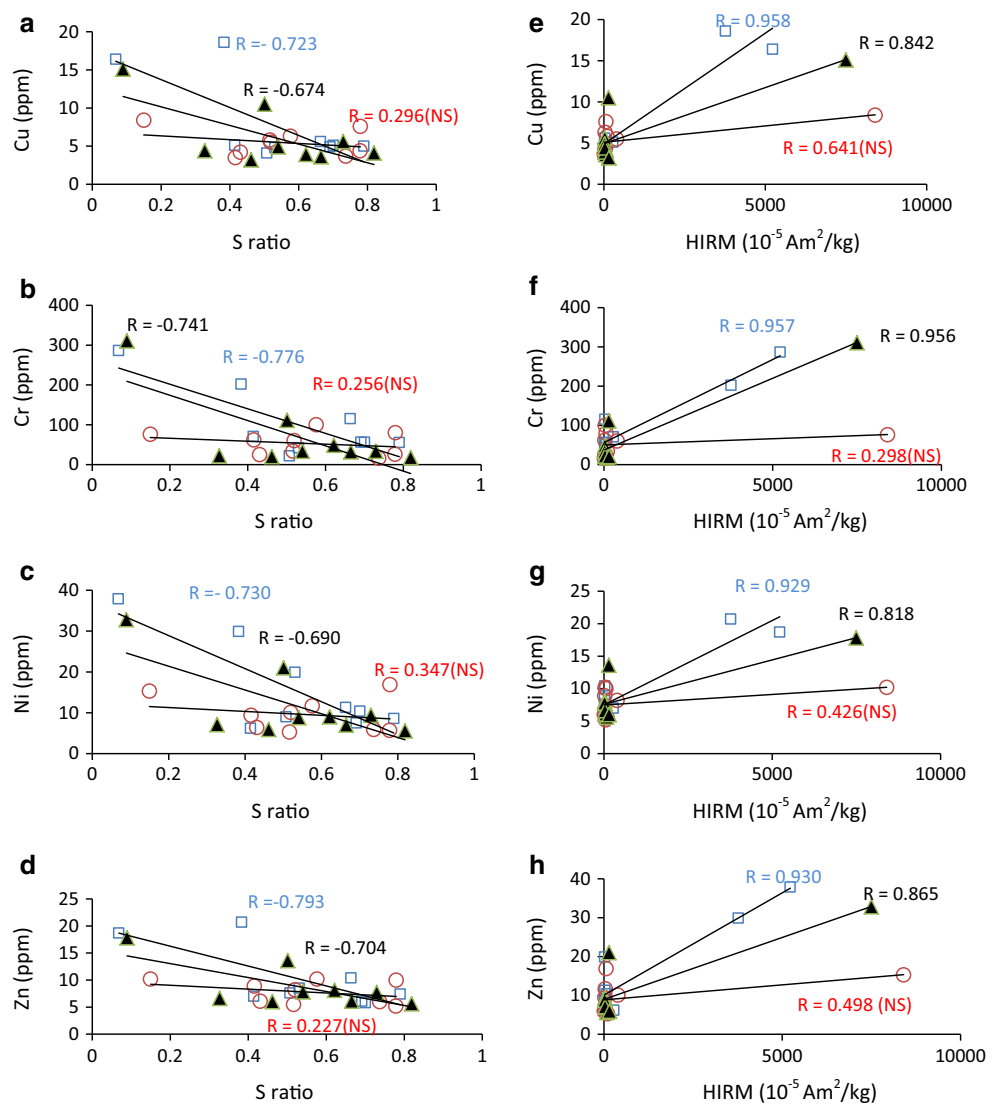
heavy metal hotspots for further detailed analyses. Magnetic parameters can thus act as proxy for heavy metals.

Conclusions

The Aravali and Vengurla beach sediments are dominated by magnetite, maghemite, titanomagnetite and hematite magnetic minerals which contain SD and MD grains. Strong correlation is evident between heavy metal con-

centration and magnetic concentration dependent parameters (χ, SIRM and HIRM) preM and PM. This correlation ceases to exist in M. Magnetic concentration dependent parameters are observed to covary with heavy metals, suggesting magnetic mineral and heavy metal input to beach sediments is from same source, especially from south of Aravali beach. The prevalence of heavy metals at Aravali is governed by geomorphological changes in the coastal tract. Significant correlation that exists between heavy metals and magnetic parameters has a huge potential

Table 3 Mineral magnetic and geochemical correlation coefficient values ($N = 27$)

	χ_{lf}	$\chi_{fd}\%$	ARM	SIRM	S ratio	HIRM	ARM/χ_{lf}	ARM/SIRM
Premonsoon								
Cu	**0.962** (0.000)	−0.631 (0.069)	0.630 (0.069)	**0.994** (0.000)	**−0.723** (0.028)	**0.958** (0.000)	**−0.704** (0.034)	**−0.803** (0.009)
Cr	**0.953** (0.000)	−0.578 (0.103)	**0.763** (0.017)	**0.926** (0.000)	**−0.776** (0.014)	**0.957** (0.000)	**−0.712** (0.031)	**−0.734** (0.024)
Ni	**0.920** (0.000)	−0.497 (0.173)	0.537 (0.136)	**0.960**** (0.000)	**−0.730** (0.025)	**0.929** (0.000)	−0.629 (0.070)	**−0.698** (0.037)
Zn	**0.907** (0.001)	−0.446 (0.229)	0.599 (0.088)	**0.907**** (0.001)	**−0.793** (0.011)	**0.930** (0.000)	**−0.680** (0.044)	**−0.696** (0.037)
Monsoon								
Cu	0.657 (0.055)	**−0.708*** (0.033)	**0.737*** (0.023)	0.653 (0.057)	−0.296 (0.440)	0.641 (0.063)	−0.578 (0.103)	0.478 (0.193)
Cr	0.353 (0.351)	−0.343 (0.366)	0.342 (0.368)	0.303 (0.428)	−0.256 (0.505)	0.298 (0.437)	−0.202 (0.602)	−0.087 (0.825)
Ni	0.459 (0.214)	−0.271 (0.481)	0.452 (0.222)	0.429 (0.249)	−0.347 (0.360)	0.426 (0.253)	−0.205 (0.597)	0.031 (0.938)
Zn	0.535 (0.138)	−0.432 (0.245)	0.583 (0.099)	0.507 (0.163)	−0.227 (0.558)	0.498 (0.173)	−0.267 (0.488)	0.171 (0.661)
Postmonsoon								
Cu	**0.833** (0.005)	−0.657 (0.055)	**0.816** (0.007)	**0.842** (0.004)	**−0.674** (0.046)	**0.842** (0.004)	−0.516 (0.155)	−0.545 (0.129)
Cr	**0.948** (0.000)	**−0.715** (0.030)	**0.905** (0.001)	**0.953** (0.000)	**−0.741** (0.022)	**0.956** (0.000)	−0.608 (0.082)	−0.518 (0.153)
Ni	**0.803** (0.009)	−0.618 (0.076)	**0.768** (0.016)	**0.813** (0.008)	**−0.690** (0.040)	**0.818** (0.007)	−0.493 (0.177)	−0.456 (0.218)
Zn	**0.852** (0.004)	**−0.668** (0.049)	**0.823** (0.006)	**0.861** (0.003)	**−0.704** (0.034)	**0.865** (0.003)	−0.522 (0.150)	−0.504 (0.166)

Correlation is significant (in bold) at the 0.05 level and derived using SPSS software. The p values of significant correlation are produced in brackets

in aiding in magnetic screening/monitoring of heavy metal pollution in coastal sediments in a rapid and cost effective manner.

References

Anderson NJ, Rippey B (1988) Diagenesis of magnetic minerals in the recent sediments of a eutrophic lake. Oceanogr, Limnol. doi:10.4319/lo.1988.33.6_part_2.1476

Arkell B, Leeks G, Newson M, Oldfield F (1983) Trapping and tracing: some recent observations of supply and transport of coarse sediment from upland Wales. Spl Publ Inte Assoc Sedimentol 6:107–119

Banerjee SK, King J, Marvin J (1981) A rapid method formagnetic granulometry with applications to environmental studies. Geophys Res Lett 8:333–336

Barron V, Torrent J (2002) Evidence for a simple pathway to maghemite in Earth and Mars soils. Geochim Cosmochim Acta 66:2801–2806

Blanchet CL, Thouveny N, Vidal L (2009) Formation and preservation of greigite (Fe3S4) in sediments from the Santa Barbara Basin: implications for paleoenvironmental changes during the past 35 ka. Paleoceanography 24:1–15

Bonnett PJP, Appleby PG, Oldfield F (1988) Radionuclides in coastal and estuarine sediments from Wirral and Lancashire. Sci Total Environ 70:215–236

Booth CA (2002) Sediment-Source-Linkages in the Gwendraeth Estuary,South Wales, based on mineral magnetic analyses. PhD thesis. University of Wolverhampton

Chan LS, Yeung CH, Yim WWS, Or OL (1998) Correlation between magnetic susceptibility and distribution of heavy metals in contaminated sea-floor sediments of Hong Kong Harbour. Environ Geol 36:77–86

Chandramohan P, Anand NM, Nayak BU (1992) Surfzone dynamics of the Konkan Coast, India. In: Desai BN (ed) Oceanography of the Indian Ocean. Oxford and IBH, New Delhi, pp 751–759

Chandrasekar N, Cherian A, Rajamanickam M, Rajamanickam GV (2003) Formation of heavy minerals in the beaches between Kallar and Vembar. Curr Sci 3(1):207–212

Chandrasekar N, Cherian A, Paul DK, Rajamanickam GV, Loveson VJ (2005) Geospatial application in the study of beach placer along the coast of Gulf of Mannar, India. Geocarta International 20(2):69–74

Chévrier V, Mathé PE, Rochette P, Gunnlaugsson HP (2006) Magnetic study of an Antarctica weathering profile on basalt: implications for recent weathering on Mars. Earth planet. Sci Lett 244:501–514

Cioppa MT, Porter NJ, Trenhaile AS, Igbokwe B, Vickers J (2010) Beach sediment magnetism and sources: Lake Erie, Ontario, Canada. J Great Lake Res 36(4):674–685. doi:10.1016/j.jglr.2010.07.007

Clifton J, McDonald P, Plater A, Oldfield F (1997) Relationships between radionuclide content and textural properties in Irish Sea intertidal sediments. Water Air Soil Pollut 99:209–216

Clifton J, McDonald P, Plater A, Oldfield F (1999) Derivation of a grainsize proxy to aid the modelling and prediction of radionuclide activity in saltmarshes and mud flats of the Eastern Irish Sea. Estuar Coast Shelf Sci 48:511–518

da Costa ACS (1996) Iron oxide minerals of soils derived from volcanic rocks in the Paraná River Basin, Brazil. Ph.D. thesis. Ohio State University

Dearing JA (1999) Susceptibility. In: Walden J, Oldfield F, Smith JP (eds) Environmental magnetism: a practical guide. Quaternary Research Association, Cambridge, pp 35–62

Deendar DI (2003) Structural controls in the formation of iron ore deposits and laterite in Vengurla area. Sustainable resource management in mining with special reference to coastal regions of Karnataka and Maharashtra. Mining Engineers Association of India, Belgaum Chapter Workshop, pp 8–10

Peters C, Dekkers, MJ (2003) Selected room temperature magnetic parameters as a function of mineralogy, concentration and grain size. Phys Chem Earth 28:659–667

Dunlop D, Ozdemir O (1997) Rock magnetism: fundamentals and frontiers. Cambridge University Press, Cambridge

Fasiska EJ (1967) Structural aspects of the oxides and oxidehydrates of iron. Corros Sci 7:833–839

Fassbinder JWE, Stanjek H (1994) Magnetic properties of biogenic soil greigite (Fe3S4). Geophys Res Lett 21:2349–2352

Fontes MPF, Weed SB (1991) Iron oxides in selected Brazilian Oxisols: I mineralogy. Soil Sci Soc Am J 55:1143–1149

Gallaway E, Trenhaile AS, Cioppa MT, Hatfield RG (2012) Magnetic mineral transport and sorting in swash-zone: Northern Lake Erie, Canada. Sedimentology doi:10.1111/j.1365-3091.2012.01323.x

Gawali PB, Basavaiah N, Hanamgond PT (2010) Mineral magnetic properties of sediments of beaches, Redi-Vengurla Coast, Central West Coast of India: a seasonal characterization and provenance study. J Coast Res 263:569–579

Gee J, Nakanishi M (1995) Magnetic petrology and magnetic properties of western Pasific guyots: implications for seamount paleopoles. Proc ODP Sci Results 144:615–630

Geiss CE, Zanner CW, Banerjee SK, Joanna M (2004) Signature of magnetic enhancement in a loessic soil in Nebraska, United States of America, Earth Planet. Sci Lett 228:355–367. doi:10.1016/j.epsl.2004.10.011

Gujar AR, Ambre NV, Mislankar PG, Sridhar D (2010) Ilmenite, magnetite and chromite beach placers from South Maharashtra, Central West Coast of India. Resour Geol 60(1):71–86

Hatfield RG, Cioppa MT, Trenhaile AS (2010) Sediment sorting and beach erosion along a coastal foreland: Magnetic measurements in Point Pelee National park, Ontario, Canada. Sed Geol 231(3–4):63–73. doi:10.1016/j.sedgeo.2010.09.007

Hegde VS, Shalini G, Kanchanagouri DG (2006) Provenance of heavy minerals with special reference to ilmenite of the Honnavar Beach, central west coast of India. Curr Sci 91(5):644–648

Heider F, Zitzelsberger A, Fabian F (1996) Magnetic susceptibility and remanent coercive force in grown magnetite crystals from 0.1 µm to 6 mm. Phys Earth Planet Int 93:239–256

Hiremath DA (2003) Iron ore deposits of Sindhudurg district Maharashtra state and their export potentiality. Sustainable resource management in mining with special reference to coastal regions of Karnataka and Maharashtra. Mining Engineers Association of India, Belgaum Chapter Workshop, pp 21–25

Hutchinson SM, Prandle D (1994) Siltation in the saltmarsh of the Dee Estuary derived from 137Cs analysis of shallow cores. Estuar Coast Shelf Sci 38:471–478

Kurian NP, Prakash TN, Jose F, Black KP (2000) Hydrodynamic processes and heavy mineral deposits of southwest coast of India. J Coastal Res 34:154–163

Lanci L, Hirt AM, Lowrie W, Lotter AF, Lemcke G, Sturm M (1999) Mineral-magnetic record of Late Quaternary climatic changes in a high Alpine lake. Earth Planet Sci Lett 170:49–59. doi:10.1016/S0012-821X(99)00098-9

Lees JA, Pethick JS (1995) Problems associated with quantitative magnetic sourcing of sediments of the Scarborough to Mablethorpe coast, Northeast England, U.K. Earth Surface Processes and Landforms 20(9):795–806. doi:10.1002/esp.3290200905

Lepland A, Stevens RL (1996) Mineral magnetic and textural interpretations of sedimentation in the Skagerrak, eastern North Sea. Mar Geol 135:51–64

Li L, Barry DA, Pattiaratchi CB, Masselink G (2002) Beach win: modeling groundwater effects on swash sediment transport and beach profile changes. Environ Model Softw 17:313–320

Maher BA, Hatfield RG (2009) Fingerprinting upland sediment sources: particle size-specific magnetic linkages between soils, lake- and suspended sediments. Earth Surf Proc Land 34:1359–1373

Maher BA, Kinnersley R (2010) Rates of particulate pollution deposition onto leaf surfaces: temporal and inter-species analyses. Environmental Pollution, p 10. doi:10.1016/j.envpol.2009.12.029

Maher BA, Kinnersley R (2011) Biomagnetic monitoring of industry-derived particulate pollution. Environ Pollut 159:1673–1681

Maher BA, Thompson R (1999) Quaternary climates, environments and magnetism. Cambridge UniversityPress

Maher BA, Pates JM, Barker PA (2008) Sediment dynamics in an upland temperate catchment: changing sediment sources, rates and deposition. J Paleolimnology 40:1143–1158

Maher BA, Watkins SJ, Brunskill G, Alexander J, Fieldings CR (2009) Sediment provenance in a tropical fluvial and marine context by magnetic fingerprinting of transportable sand fractions. Sedimentology 5:841–861

Murad E, Schwertmann U (1993) Temporal stability of a finegrained magnetite. Clays Clay Miner 41:111–113

Oldfield F (1999a) Environmental magnetism; the range of applications. In: Walden J, Smith JP, Oldfield F (ed) Environmental magnetism, a practical guide, quaternary research association. Technical Guide 6:212–22

Oldfield F (1999b) The rock magnetic identification of magnetic mineral and grain size assemblages. In: Walden J, Smith JP, Oldfield F (ed) Environmental magnetism, a practical guide, quaternary research association. Technical Guide 6:98–112

Oldfield F, Richardson N (1990) Lake sediment magnetism and atmospheric deposition. Philos T R Soc B327:325–330

Oldfield F, Yu L (1994) The influence of particle size variations on the magnetic properties of sediments from the north-eastern Irish Sea. Sedimentology 41:1093–1108

Oldfield F, Maher BA, Donoghue J, Pierce J (1985) Particle size related, mineral magnetic source sediment linkages in the Rhode River catchment, Maryland, USA. J Geol Soc (London) 142:1035–1046

Oldfield F, Richardson N, Appleby PG, Yu L (1993) ^{241}Am and ^{137}Cs activity in fine grained salt marsh sediments from parts of the NE Irish Sea shoreline. J Environ Radioact 19:1–24

Oldfield F, Appleby PG, van der Post KD (1999) Problems of core correlation, sediment source ascription and yield estimation in Ponsonby Tarn, West Cumbria, UK. Earth Surf Processes Land 24:975–992

Petrovsky E, Kapicka A, Zapletal K, Sebestova E, Spanila T, Dekkers MJ (1998) Correlation between magnetic parameters and chemical composition of lake sediments from NorthernBohemia—Preliminary Study. Phys Chem Earth 23:1123–1126

Roberts AP, Chang L, Rowan CJ, Horng CS, Florindo F (2011) Magnetic properties of sedimentary greigite (Fe3S4): an update. Rev. Geophys. 49:RG1002

Schmidt AM, Von Dobeneck T, Bleil U (1999) Magnetic characterization of Holocene sedimentation in the South Atlantic. Palaeoceanography 14:465–481

Schwertmann U, Heinemann B (1959) Uber das Vorkommen und die Entstehung von Maghemit in nordwest deutschen Böden, Neues Jahrb. Miner Monatsh 8:174–181

Tandale TD (1993) Coastal environ of Maharashtra: evolution and human activities aided with satellite remote sensing. Photonir-vachak 21(2):59–65

Thompson R, Oldfield F (1986) Environmental Magnetism. Unwin and Allen, London

Turner GM (1997) Environmental magnetism and magnetic correlation of high resolution lake sediment records from Northern Hawkés Bay, New Zealand. J Geol Geophys 40:287–298

van der Marel HW (1951) Ferric oxide in sediments. J Sed Petrol. 21:12–21

Walden J, Smith JP, Dackombe RV, Rose J (1995) Mineral magnetic analyses of glacial diamicts from the Midland Valley of Scotland. Scott J Geol 31:79–89

Walden J, Slattery MC, Burt TP (1997) Use of mineral magnetic measurements to fingerprint suspended sediment sources: approaches and techniques for data analysis. J Hydrol 202:353–372

Walden J, Smith JP, Oldfield F (1999) Environmental magnetism, a practical guide. Quaternary research association. Technical Guide 6:243

Wheeler AJ, Oldfield F, Orford JD (1999) Sedimentology and postdepositional controls on magnetic signals from saltmarshes on the north-west coast of Ireland. Sedimentology 46:545–558

White K, Walden J, Drake N, Eckardt F, Settle J (1997) Mapping the iron oxide content of dune sands, Namib Sand Sea, Namibia, using Landsat Thematic Mapper data. Remote Sens Environ 62:30–39

Xie S, Dearing JA, Bloemandal J, Boyle JF (1999) Association between the organic matter content and magnetic properties in street dust, Liverpool, UK. Sci Total Environ 241:205–214

Xie S, Dearing JA, Bloemandal J (2000) The organic matter content of street dust in Liverpool, UK and its association with dust magnetic properties. Atmos Environ 34:225–269

Zhang W, Yu L, Hutchinson SM (2001) Diagenesis of magnetic minerals in the intertidal sediments of the Yangtze Estuary, China, and its environmental significance. Sci Total Environ 266:160–175